

# An Estimation Method for the SLF/ELF Field Strength with L-type Horizontal Line-Current Antennas over Inhomogeneous Anisotropic Ground

Bin Li<sup>1,2</sup>, Chao Liu<sup>2</sup>, Hua-ning Wu<sup>2</sup>, and Bo Zhang<sup>3</sup>

<sup>1</sup> National Key Laboratory of National Defense Technology for Integrated Ship Power Technology  
Naval University of Engineering, Wuhan, 430033, China  
libin521002@sina.com

<sup>2</sup> Department of Electronic Engineering  
Naval University of Engineering, Wuhan, 430033, China  
chaoliunue@sina.com, wuhuaning007@163.com

<sup>3</sup> Naval Academy of Armament  
Shanghai, 200436, China  
zbdtc123123@sina.com

**Abstract** — In this study, the radiation characteristics of the control source of extremely low frequency (CSELF) horizontal line-current antennas are studied by the reciprocity theorem. The radiation field strength expressions of the CSELF L-type horizontal line-current antenna are derived on the basis of a field-direction coefficient in the spherical earth-ionosphere cavity. The estimation results of the super low frequency/extremely low frequency (SLF/ELF) wave are provided with regard to the conductivity, the propagation distances and the water-depth. The propagation characteristics of the CSELF wave are calculated under different conditions and are compared to Bannister's method. The effectiveness of the proposed method is validated by a case study.

**Index Terms** — Control source of extremely low frequency (CSELF), earth-ionosphere cavity, ground resistivity, horizontal dipole antenna.

## I. INTRODUCTION

The control source of extremely low frequency (CSELF) method is a key technique for underwater communications and electromagnetic exploration [1-4], especially for earthquake prediction and oil and gas exploration. Compared with other electromagnetic detection technologies, SLF/ELF detection has greater advantages regarding the detecting depth and precision and can be applied to geomagnetic high-energy radiation and underground exploration fields [5, 6]. The effective radiation of the SLF/ELF electromagnetic wave is a crucial component of the CSELF method. Horizontal line-current antennas have been implemented extensively as effective transmitting antennas in the

SLF/ELF band. As shown in Fig. 1, a horizontal line-current antenna is low-slung in a high ground resistivity region, and grounding electrodes are at the two ends of the cable, which transmits a sinusoidal alternating current underground. Thus, a huge amperage current loop is formed by the tens of kilometers of the cables and the ground currents. For a long dipole horizontal antenna with fixed length at a specific frequency, an antenna ground with high equivalent resistivity can enhance the effective skin depth. The magnetic moment of the current loop is large, which is equivalent to increasing the electrical size of the line-current antenna. Therefore, the horizontal line antenna can be seen as a horizontal magnetic dipole (HMD) in the Earth-ionosphere cavity [7, 8].

Generally, the apparent resistivity of the control source station affects the radiation characteristics of the ELF electromagnetic waves in the Earth-ionosphere cavity. A high ground resistivity in the antenna path area is an important factor to improve the performance of the SLF/ELF transmission system [9]. The crust is affected by geological structures such as bedrock strike, gullies, and fault zones. Hence, the resistivity of the earth's crust is actually anisotropic and inhomogeneous [10]. Due to the constraint of the geological structure, CSELF horizontal line-current antennas, which may have a length of up to tens of kilometers, usually consist of several L-type folded lines. Many numerical analyses have focused on the geo-electric magnetic field strength (MFS) and the distribution of the surface-induced electric field strength (EFS) of the horizontal electric dipole (HED) [11-13]. However, the radiation field of the L-type horizontal line-current antenna over inhomogeneous anisotropic ground has not received

sufficient attention, especially in the ocean environment. Therefore, this study focuses on the radiation field of the CSELF and proposes a low-complexity estimation method for the field intensity of the L-type horizontal line-current antenna over inhomogeneous anisotropic ground based on the waveguide theory. Solving the radiation field of the SLF/ELF provides an approximate solution for remote sensing of the underground and underwater environment.

This paper is organized as follows. Section 2 briefly describes the electrical characteristics of the horizontal line-current antenna path and proposes the closed-form solution for the CSELF radiation field of the L-type horizontal line-current antenna. In Section 3, we present the calculated results and illustrate the radiation characteristics of the CSELF L-type horizontal line-current antenna. The conclusions of this paper are presented in Section 4.

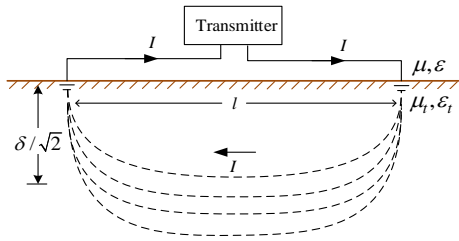


Fig. 1. A horizontal line-current antenna grounded at each end.

## II. ANALYTICAL FORMULAS FOR THE CSELF RADIATION FIELD

### A. The electrical characteristics of the CSELF antenna path

Generally, the surface geometries of the antenna path have no significant influence on the SLF/ELF propagation. However, the conductivities of the CSELF antenna path from the land surface to a certain depth have a great effect on the propagation of the SLF/ELF electromagnetic wave [14]. Therefore, it is necessary to study the electrical characteristics of the CSELF antenna path. As part of the input resistance, the resistance of the ground loss determines the CSELF radiation efficiency of the horizontal L-type line-current antenna. In most of the medium models, the resistivity of the ground is represented by the horizontal layered structure or the half-space homogeneous structure [15-18].

A SLF/ELF electromagnetic wave has a deeper skin depth underground. Hence, it cannot be considered that the electrical properties of the ground are homogeneous. In a Cartesian coordinate system, the vertical plane waves propagate vertically downward (along the positive z-axis). When the time variation factor is set as  $e^{j\omega t}$ , the electromagnetic waves can be expressed in the x-axis direction [19]:

$$\partial^2 E_x / \partial z^2 - k^2 E_x = 0. \quad (1)$$

$k^2 \approx -j\omega\mu_{xl}\sigma_{xl}$ ,  $\omega$  denotes the angular frequency,  $\mu_{xl}$  denotes the permeability tensor element, and  $\sigma_{xl}$  denotes the conductivity tensor element. When z is infinite, the general solution of Equation (1) is:

$$E_x = Ae^{-kz}. \quad (2)$$

A denotes a constant. Based on the differential formula of Faraday's law  $\nabla \times \mathbf{E} = -j\omega\boldsymbol{\mu} \cdot \mathbf{H}$ ; the component of the MFS in the direction of the y-axis can be obtained by:

$$H_y = -\frac{A}{\sqrt{j\omega\mu_{xl}\rho_{xl}}} e^{-kz}. \quad (3)$$

Using Equations (2) and (3), the impedance of the plane wave can be represented as:

$$\eta_{xy} = -\sqrt{j\omega\mu_{xl}\rho_{xl}} \cdot e^{-j\pi/4}. \quad (4)$$

$\rho_{xl}$  denotes the ground equivalent resistivity along the x-axis. It can be seen that the wave impedance is closely related to the resistivity and the ground equivalent resistivity can be determined by the magnetotelluric method [20].

### B. The estimation method for the CSELF in the Earth-ionosphere cavity

The total path of the SLF/ELF long dipole antenna with high power can reach hundreds of kilometers. The L-type emission source has a higher resolution than the horizontal long loop source and the ring source [21]. The ionosphere disturbances have a great influence on the amplitude and phase of the ELF/very low frequency (VLF) electromagnetic wave [22-24]. Using a horizontal line-current antenna as a model, other forms of artificial sources can be made up of multiple horizontal antennas. We regard the horizontal line-current antenna as a HED in the Earth-ionosphere cavity. The radiation field of the electric dipole is a transverse magnetic (TM) wave. For an observer located in the far field, the relative wave-number is  $k_r \geq 1$ . The effective reflection height of the ionosphere to the SLF/ELF wave is far less than the wavelength of the SLF/ELF wave in free space. The MFS component  $\mathbf{H}_r$  is very small and negligible compared to the  $\mathbf{H}_\theta$  component and the  $\mathbf{H}_\phi$  component; therefore, the SLF/ELF electromagnetic wave is a transverse electromagnetic (TEM) wave in the far field.

In a flat earth-ionosphere cavity, the vertical EFS component of the short vertical current source on the ground can be obtained from the perpendicular EFS component of a line-current source, which is in an infinite medium, with an infinite length and a uniform line as in the following:

$$E_z(\rho) = -\frac{\omega\mu_e I l}{4h_i} H_0^{(2)}(Sk_0\rho). \quad (5)$$

I denotes the antenna current, l denotes the length of the short vertical current source,  $h_i$  denotes the ionosphere

height, and  $H_0^{(2)}(Sk_0\rho)$  denotes the second kind of the Hankel function.

As shown in Fig. 2, the horizontal line-current source  $Il_1$  and  $Il_2$  are placed on the surface of the earth in a Cartesian coordinate system, and the source  $Il_1$  points in the positive direction of the x-axis which originates from the coordinate origin  $o$ . The experimental vertical electrical dipole (VED) source is placed at the point  $o'$ . When the principal axis of the surface impedance is regarded as the normal direction of the  $x'o'y'$  plane in a Cartesian coordinate system,  $\varphi$  denotes the angle between the radial direction and the x-axis and  $\varphi'$  denotes the angle between the radial direction and the  $x'$ -axis. The two sources are set in the same space. According to the reciprocity theorem [12, 19], the electromagnetic field produced by the horizontal line-current sources and the VED satisfies:

$$\int_l \mathbf{E} \cdot \hat{\mathbf{r}} I_1 dl_1 = \int_l \mathbf{H} \cdot \hat{\mathbf{y}} I' dl'. \quad (6)$$

Based on Equation (6), in the flat earth-ionosphere cavity, the vertical EFS component of the current source is given as:

$$E_z' = -E_\rho \cos \varphi' = \eta_g H_\phi \cos \phi'. \quad (7)$$

$E_\rho$  denotes the horizontal EFS at  $Il_1$ , produced by the vertical current source  $I'l'$ . In the Earth-ionosphere cavity, we assume  $I'l' = Il_1$ . When the distance  $\rho$  between the field point and source point is greater than the ionosphere height  $h_i$ , the location of the field point is not near the antipodal point. Based on Equations (5) and (7), the radial EFS of the direct wave can be expressed as follows:

$$E_r^d = -j \frac{II S k_0}{4h_i} \left( \frac{\omega \mu \rho_g}{j} \right)^{1/2} \cdot \left[ \frac{\rho/a_e}{\sin(\rho/a_e)} \right]^{1/2} H_1^{(2)}(Sk_0\rho) \cos \varphi. \quad (8)$$

$\left[ \frac{\rho/a_e}{\sin(\rho/a_e)} \right]^{1/2}$  denotes the spherical focusing factor. Using the Maxwell equation, the magnetic field in a spherical cavity can be obtained as follows:

$$\mathbf{H}^d = -\frac{II S k_0}{4h_i \eta_e} \left( \frac{\omega \mu \rho_g}{j} \right)^{1/2} \left[ \frac{\rho/a_e}{\sin(\rho/a_e)} \right]^{1/2} \left\{ \hat{\theta} \frac{1}{Sk_0\rho} \cdot H_1^{(2)}(Sk_0\rho) \sin \varphi + \hat{\phi} \cdot \left[ H_0^{(2)}(Sk_0\rho) - \frac{1}{Sk_0\rho} H_1^{(2)}(Sk_0\rho) \right] \cos \varphi \right\}. \quad (9)$$

$k_0$  is the wave number,  $a_e$  is the earth radius, and  $S$  is the parameter of the cavity. Similarly, the EFS and MFS of the direct wave of the source  $Il_2$  can be obtained by Equations (8) and (9). However, the field opponent differs for the source  $Il_2$  and the source  $Il_1$  due to the folded angle. The field-direction coefficient can be expressed as follows:

$$S_f \approx \begin{cases} (\cos \varphi + \cos(\pi - \gamma_n - \varphi)), & 0 \leq \varphi \leq \pi/2. \\ (\cos \varphi + \cos(\pi - \gamma_n + \varphi)), & -\pi/2 \leq \varphi < 0. \end{cases} \quad (10)$$

$\gamma_n$  denotes the folded angle of the  $n$ th fold line between the radial direction and the positive x-axis. We assume that the angle  $\gamma$  is in the range of  $[\pi/2, 3\pi/2]$ . The waves of the multiple circulations are negligible because of the attenuation in the cavity. Using the approximate expression of the Hankel function, we simplify the EFS expression of the L-type line-current antennas as:

$$|(E_r)^d| \approx \frac{fI}{2h_i} \left( \frac{2\pi\mu}{c_0} \right)^{1/2} \cdot \left[ \frac{\rho}{a_e} \right]^{1/2} \frac{e^{-\alpha\rho}}{(\rho \frac{c_0}{v_p})^{1/2}} \left[ \begin{aligned} & l_1 \sqrt{\rho_{gn}} \cos \varphi - \sum_{n=2}^m l_n \sqrt{\rho_{gn}} \\ & \cdot \begin{cases} \cos(\gamma_{n-1} - \varphi), & -\pi/2 \leq \varphi \leq 0, \\ \cos(\gamma_{n-1} + \varphi), & 0 \leq \varphi \leq \pi/2, \end{cases} \end{aligned} \right], \quad (11)$$

where  $l_n$  and  $\rho_{gn}$  denote the length and the equivalent ground resistivity respectively of the  $n$ th fold line,  $c_0$  denotes the speed of light in a vacuum, and  $v_p$  denotes the wave velocity in the waveguide. The approximate expressions for the radial magnetic field strength can be derived from the wave impedance and Equation (11), which is similar to Bannister's expression [25]. According to Equation (11), when the length of the antenna is determined, the electrical parameter that determines the radiation capability of the CSELF antenna is mainly the ground resistivity of the antenna path.

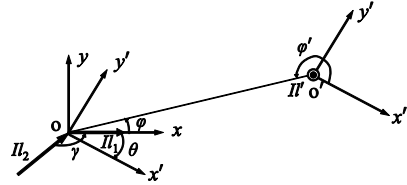


Fig. 2. Reciprocal relationship between an L-type line-current antenna and a VED.

### III. NUMERICAL RESULTS AND DISCUSSION

In this section, the characteristics of the radiation field of the CSELF antenna are simulated in detail. As shown in Fig. 3, using an L-type horizontal antenna as an example, we assume that the CSELF horizontal L-type line-current antenna is placed in the xoy plane. The lengths of the two L-type lines are  $l_1 = 80$  km and  $l_2 = 120$  km. The first L-type line is parallel to the x-axis. The fold angle is  $\gamma = 150^\circ$ . A horizontal line antenna with an equivalent length is placed on the x-axis and is calculated by Bannister's method for comparison. A homogeneous ground with a resistivity of  $5000 \Omega$  is selected as the ground dielectric model. The alternating current of the artificial source is 300 A and the operating

frequencies are 70 Hz and 130 Hz, respectively. The effective reflection height of the ionosphere is 75 km.

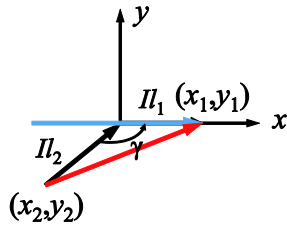
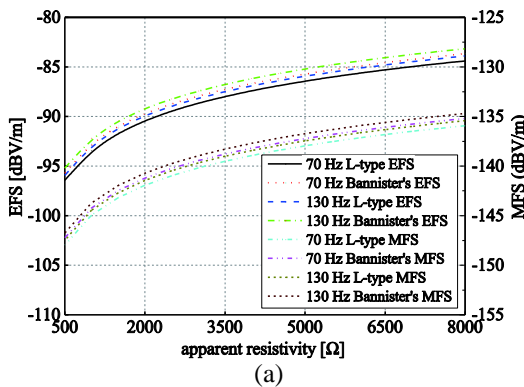
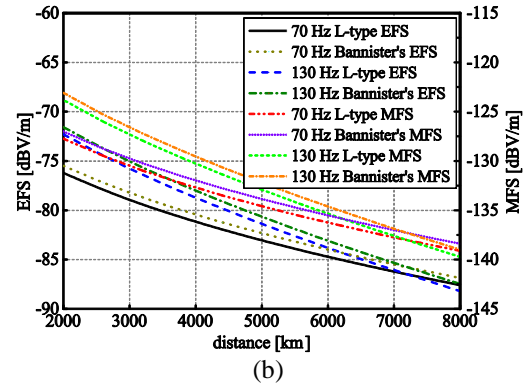


Fig. 3. Simulation model of the L-type line-current antenna.

The field strength values of the antenna are shown in Fig. 4. Figure 4 (a) indicates that the EFS and MFS of the CSELF are increasing with increasing values of the apparent resistivity at 7000 km. Compared with the EFS and MFS values of the horizontal line antenna, the fold line antenna has a lower field strength value. When the apparent resistivity is above 5000  $\Omega$ , the field strength values of the CSELF source do not increase considerably and the differences in the field strength are less than 3 dBV/m in the far field. Therefore, a high apparent resistivity improves the field strength of the CSELF source. The frequencies have little effect on the field strength in the SLF/ELF band. Figure 4 (b) shows that the field strength of the CSELF decreases as the propagation distance increases in the Earth-ionosphere cavity. With a decrease in the frequency, the initial EFS decreases and the decay rate of the field strength decreases slightly. Hence, within 7000 km, the higher-frequency portion of the SLF/ELF wave is better suited for communication purposes. Beyond 7000 km, the low-frequency portion of the SLF/ELF should be used to obtain relatively higher signal strength. Near the air-seawater interface, the wave on the interface is dominated by the vertical electric field component. The communication at sea depends mainly on the horizontal component of the field strength.



(a)



(b)

Fig. 4. (a) EFS and MFS of the CSELF versus apparent resistivity at  $x=7000$  km, and (b) EPS and MFS of the CSELF versus the distance.

Figure 5 (a) shows the horizontal component of the EFS with respect to the propagation distance. Compared with the EFS values in Fig. 4 (b), the field strength values of the waves are strongly attenuated by four orders of magnitude at the air-seawater interface. Figure. 5 (b) shows that the EFS values of the CSELF are decreasing with increasing depth. When the SLF/ELF wave propagates in the single-mode region of the Earth-ionosphere cavity (2000–8000 km), the higher the frequency is, the faster the attenuation and the lower the penetration depth is. The EFS horizontal component of the SLF/ELF waves exhibits slight differences in shallow water. However, when the SLF/ELF wave signals are transmitted to a larger depth, a lower frequency is required. Considering the limited capacity of the channel, maintaining a balance between the penetration and the communication capability represents a problem of shore based CSELF in underwater communications.

The simulations indicate that the results of the proposed method are basically consistent with the results of the Bannister's expression. We believe that these consistencies are mainly caused by the waveguide theory and the similar simulation environments. The field strength of the fold line antenna is relatively smaller than the field strength derived by Bannister's expression. Because the fold line antenna is equivalent to the dipole signed by the red dotted line in Fig. 3, the  $\varphi$  angle is larger for the equivalent antenna than for the compared antenna. Moreover, the ground conductivity is assumed as the homogenous ground in the above case. The numerical solution of the fold line antennas can be obtained by the equivalent antenna. Therefore, the equivalent conductivity is regarded as a practical solution procedure of the inhomogeneous anisotropic ground conductivity. Note that these simulation results

are obtained under specific conditions (earth-ionosphere cavity) and that the effect of inhomogeneous anisotropic ground conductivity on the L-type line-current antenna requires further study.

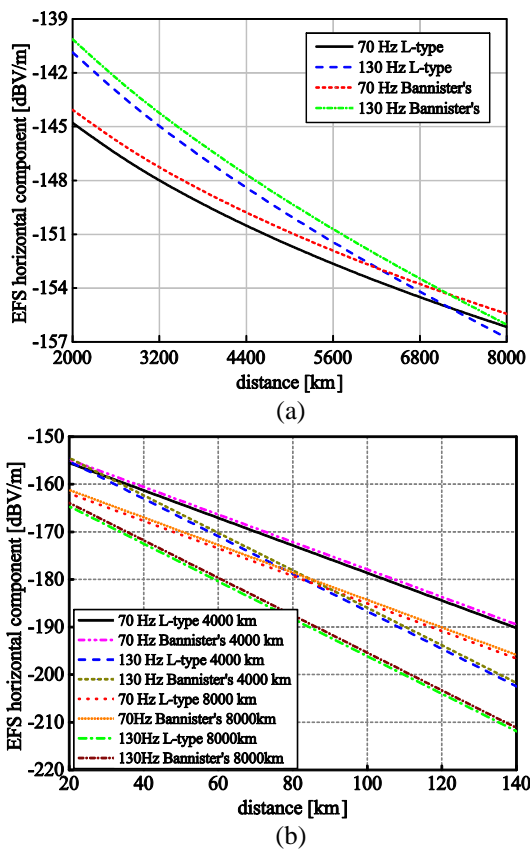


Fig. 5. (a) EFS horizontal component of the CSELF versus distance at the air-seawater interface, and (b) EPS horizontal component of the CSELF versus sea-water depth.

#### IV. CONCLUSIONS

In this study, the radiation characteristics of the CSELF in the Earth-ionosphere cavity are investigated and a novel low-complexity estimation method for the CSELF with an L-type horizontal line-current antenna is proposed. Using the reciprocity theorem, the EFS and MFS closed-form expressions of the CSELF are given in a spherical earth-ionosphere cavity. A simulation of the proposed closed-form solution shows that the ground resistivity of the control source station has a large effect on the SLF/ELF field intensity in the far field. A high apparent resistivity improves the field strength of the CSELF source. When the SLF/ELF waves pass from the air to the water, the SLF/ELF waves are attenuated strongly by the seawater surface. The higher the frequency, the smaller the penetration depth is. It is verified by a theoretical analysis and simulations that the proposed estimation method predicts the field strength of

the CSELF accurately.

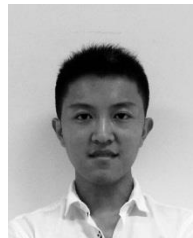
#### ACKNOWLEDGMENT

This work was supported by the National Nature Science Foundation of China (Grant Nos. 41727804).

#### REFERENCES

- [1] S. Coco, A. Laudani, F. R. Fulginei, and A. Salvini, "A new neural predictor for ELF magnetic field strength," *IEEE Transactions on Magnetics*, vol. 50, no. 2, pp. 69-72, Feb. 2014.
- [2] G. Lucca, "Analytical evaluation of sub-sea ELF electromagnetic field generated by submarine power cables," *Progress in Electromagnetics Research B*, vol. 56, pp. 309-326, Dec. 2013.
- [3] N. Damiano, L. Yan, B. Whisner, and C. Zhou, "Simulation and measurement of through-the-earth (TTE), extremely low-frequency signals using copper-clad, steel ground rods," *IEEE Transactions on Industry Applications*, vol. 53, no. 5, pp. 5099-5095, Sept.-Oct. 2017.
- [4] Y. Wang, Y. Zhou, and Q. S. Cao, "Study of ELF propagation parameters based on the simulated Schumann resonances," *IEEE Antennas and Wireless Propagation Letters*, vol. 13, pp. 63-66, Dec. 2013.
- [5] K. Shiokawa, Y. Yokoyama, A. Ieda, Y. Miyoshi, et al., "Ground-based VLF/ELF chorus observations at subauroral latitudes - VLF-CHAIN campaign," *Journal of Geophysical Research Space Physics*, vol. 119, no. 9, pp. 7363-7379, Sept. 2015.
- [6] G. Z. Zhao, L. F. Wang, J. Tang, X. B. Chen, et al., "New experiments of CSELF electromagnetic method for earthquake monitoring," *Chinese Journal of Geophysics*, vol. 53, no. 3, pp. 479-486, Mar. 2010.
- [7] C. Liu, B. Wang, H. Q. Xu, and Y. L. Liu, "The impedance characteristics of ELF line-current antenna over inhomogeneous anisotropic ground," *Applied Mechanics and Materials*, vol. 548-549, pp. 771-775, June 2014.
- [8] M. L. Burrows and C. W. Niessen, "ELF communication system design," *Engineering in the Ocean Environment, Ocean 72 - IEEE International Conference on*, Newport, RI, pp. 95-109, Sept. 1972.
- [9] M. L. Burrows, "Surface impedance and the efficiency of horizontal-dipole extremely low frequency (ELF) antenna arrays," *IEEE Transactions on Communications*, vol. 22, no. 4, pp. 475-483, Apr. 1974.
- [10] W. D. Xu, X. M. Zhang, Z. Li, S. F. Zhao, and W. Zhang, "Statistical analysis of the propagation characteristics of VLF electromagnetic waves excited by the artificial transmitter," *Chinese*

- Journal of Geophysics*, vol. 59, no. 5, pp. 1578-1584, May 2016.
- [11] Y. X. Wang, R. H. Jin, J. P. Geng, and X. L. Liang, "Exact SLF/ELF underground HED field strengths in earth-ionosphere cavity and Schumann resonance," *IEEE Transactions on Antennas and Propagation*, vol. 59, no. 8, pp. 3031-3039, Aug. 2011.
- [12] C. Liu, L. G. Zheng, and Y. P. Li, "A closed-form solution for ELF radiated fields of a line-current antenna in earth-ionosphere waveguide," *International Conference on Wireless Communications, Networking and Mobile Computing*, Beijing, pp. 2506-2509, Sept. 2009.
- [13] M. Hayakawa and T. Otsuyama, "FDTD analysis of ELF wave propagation in inhomogeneous subionospheric waveguide models," *Applied Computational Electromagnetics Society Journal*, vol. 17, no. 3, pp. 239-244, Nov. 2002.
- [14] S. V. Makki, T. Z. Ershadi, and M. S. Abrishamian, "Determining the specific ground conductivity aided by the horizontal electric dipole antenna near the ground surface," *Progress in Electromagnetics Research B*, vol. 1, pp. 43-65, Jan. 2008.
- [15] A. Kulak and J. Mlynarczyk, "ELF propagation parameters for the ground-ionosphere waveguide with finite ground conductivity," *IEEE Transactions on Antennas and Propagation*, vol. 61, no. 4, pp. 2269-2275, Apr. 2013.
- [16] D. L. Paul and C. J. Raitlon, "Spherical ADI FDTD method with application to propagation in the earth ionosphere cavity," *IEEE Transactions on Antennas and Propagation*, vol. 60, no. 1, pp. 310-317, Jan. 2012.
- [17] G. Lucca, "Analytical evaluation of sub-sea ELF electromagnetic field generated by submarine power cables," *Progress in Electromagnetics Research B*, vol. 56, pp. 309-326, Dec. 2013.
- [18] H. Y. Li, J. Zhan, Z. S. Wu, and P. Kong, "Numerical simulations of ELF/VLF wave generated by modulated beat-wave ionospheric heating in high latitude regions," *Progress in Electromagnetics Research M*, vol. 50, pp. 55-63, Jan. 2016.
- [19] Y. P. Wang, *Engineering Electrodynamics*, Xidian University Press, Xi'an, 2007.
- [20] P. S. Greifinger, V. C. Mushtak, and E. R. Williams, "On modeling the lower characteristic ELF altitude from aeronautical data," *Radio Science*, vol. 42, no. 2, pp. 1-12, Apr. 2007.
- [21] C. M. Fu, Q. Y. Di, C. Xu, and M. Y. Wang, "Electromagnetic fields for different type sources with effect of the ionosphere," *Chinese Journal of Geophysics*, vol. 55, no. 12, pp. 3958-3968, Dec. 2012.
- [22] M. S. Zhdanov, *Geophysical Electromagnetic Theory and Methods*, Elsevier Science, New York, 2009.
- [23] T. B. Jones, K. Davies, and B. Wieder, "Observations of D region modification at low and very low frequencies," *Nature*, vol. 238, no. 5358, pp. 33-34, Jul. 1972.
- [24] G. Z. Li, T. T. Gu, and K. Li, "SLF/ELF electromagnetic field of a horizontal dipole in the presence of an anisotropic earth-ionosphere cavity," *Applied Computational Electromagnetics Society Journal*, vol. 29, no. 12, pp. 1102-1111, Dec. 2014.
- [25] P. R. Bannister, "ELF propagation update," *IEEE Journal of Oceanic Engineering*, vol. oe-9, no. 3, pp. 179-188, Jul. 1984.



**Bin Li** received his M.S. and Ph.D. degrees from Naval University of Engineering, Wuhan, China, in 2015 and 2019.

He currently serves as a Research Assistant at Naval University of Engineering. His current research interests include SLF/ELF wave

propagation and electromagnetic interference.



**Chao Liu** received the M.S. and Ph.D. degrees in Electromagnetic Field and Microwave Technology from Xidian University, Xi'an, China.

He was a Professor at Naval University of Engineering. His research interests include VLF communication, antenna design and numerical analysis for electromagnetic fields.



**Hua-ning Wu** received his M.S. and Ph.D. degrees from Naval University of Engineering, Hubei, China, in 2012 and 2015.

He currently serves as a Lecturer at Naval University of Engineering. His research interests include antenna array pattern

synthesis, intelligent antenna design.



**Bo Zhang** received his M.S. degree from Naval University of Engineering, Hubei, China, in 2015.

He currently served as an Engineer at Naval Academy of Armament. His research interests include electronic control and circuit design, intelligent antenna

design.